Article

Titanium Dioxide–Reduced Graphene Oxide Composites for Photocatalytic Degradation of Dyes in Water

Lei Yu [1,2], Wenlong Xu [2,3], Huie Liu [2,*] and Yan Bao [3,*]

1 Binzhou Institute of Science and Technology Innovation and Development, Binzhou 256600, China
2 State Key Laboratory of Heavy Oil Processing, College of Chemical Engineering, China University of Petroleum (Huadong), Qingdao 266580, China
3 Qingdao Institute of Bioenergy and Bioprocess Technology, Chinese Academy of Sciences, Qingdao 266101, China
* Correspondence: liuhuie@upc.edu.cn (H.L.); baoyan@qibebt.ac.cn (Y.B.); Tel.: +86-15953220936 (H.L.); +86-0532-80662718 (Y.B.)

Abstract: Dye wastewater due to industrialization, urbanization and academic activities has become one of the most important environmental issues today. Photocatalytic degradation technology is considered as a promising technology for treating dye wastewater due to its advantages of environmental protection and low energy consumption. Herein, titanium dioxide–reduced graphene oxide composites (TiO_2-RGO) were prepared by a one-step hydrothermal method to degrade different dyes (methyl orange, methylene blue and rhodamine B) in water. The structure and morphology of TiO_2-RGO were characterized using various technical approaches. The degradation effect of TiO_2-RGO on the dye was in accordance with a first-order kinetic reaction. The degradation rate of TiO_2-6%RGO for methyl orange at 15 min was 1.67 times higher than that of TiO_2, due to the strong electron transport ability and excellent adsorption properties of graphene. TiO_2-6%RGO has better degradation performance for fluorescent dyes and anionic azo dyes. Notably, the degradation rate of methyl orange by TiO_2-6%RGO photocatalysis for 90 min could reach 96.9%. Meanwhile, the TiO_2-6%RGO showed excellent reusability, as the initial degradation rate of 93.2% was maintained after five degradation cycles of methyl orange solution. The present work provides a universal strategy for designing efficient photocatalytic materials.

Keywords: photocatalytic; dye degradation; titanium dioxide; reduced graphene oxide

1. Introduction

The treatment of dye wastewater has been a pressing problem in the environmental field due to its deep coloration, stable properties and complex structure. For example, azo anionic dyes, such as methyl orange, which is commonly used as an acid–base indicator, methylene blue, a cationic dye commonly used in the printing and dyeing industry, and rhodamine B, a fluorescent dye widely used in colored glass, may pose a serious threat to ecosystems and human health even at very low concentrations of emissions during production and use. The methods commonly used to remove dyes from water can be divided into physical, chemical and biological methods according to the mechanism of the treatment process [1–4]. Physical methods mainly use machines to treat sewage, and commonly used methods include centrifugal separation, sedimentation, and filtration. These methods only extract the pollutants in the water, but cannot completely eliminate the pollutants. Chemical methods commonly use electrical treatment, chemical precipitation treatment, oxidation treatment, etc., to treat pollutants dissolved in water. The chemical reagents used in this method are expensive and produce sludge that is difficult to dewater after treatment. The biological method mainly uses microbial metabolism to control water pollution. This method has strong pertinence and poor treatment effect in situations where the water contains various pollutants. It is not universal, and it is difficult to popularize and

apply on a large scale. Therefore, finding an efficient, environmentally friendly, economical and feasible universal water pollution control method is the key to solving the problem of sewage treatment.

In recent years, photocatalytic technology has attracted the attention of many researchers due to its advantages of environmental protection and low energy consumption [5–9]. This method can convert a variety of organic pollutants into clean water, carbon dioxide and other substances without recontamination, thus completely solving the problem of organic contamination, such as dyes cause in water. Among the wide variety of photocatalysts (TiO_2, MoS_2 SnO_2, Fe/C_3N_4, $Ag/AgCl/ZnTiO_3$, CdS, etc. [10–15]), TiO_2 is the material of choice for research because of its stable optical properties, low price, abundant precursors, and simple preparation. However, TiO_2 suffers from defects such as a wide band gap and easy recombination of electron–hole pairs. At present, there are two main methods to improve TiO_2 defects: one is to adjust the band gap, particle size and crystal surface of TiO_2 by changing its preparation conditions; the other is to improve its photocatalytic performance by compounding with other materials [16–20].

Graphene has a strong electron transport ability, and its theoretical electron mobility is about 200,000 $cm^2 \cdot V^{-1} \cdot s^{-1}$ at room temperature. Using this ability, the photogenerated electrons generated by the excitation of light on the valence band of TiO_2 can be quickly transferred, thereby inhibiting the recombination of photogenerated electrons and holes and reducing the loss of light energy [21,22]. In addition, graphene also has a strong adsorption capacity, which can improve the contact probability of pollutants and photocatalytic active components when it is prepared into a photocatalytic composite material, thereby further improving the photocatalytic performance of the composite material. Tang et al. [23] prepared $TiO_2/Ag/rGO$ heterogeneous nanocomposites in two steps by introducing silver and graphene into TiO_2 nanowires, and used them to degrade rhodamine B in water with good degradation results. Wang et al. [24] prepared titanium dioxide @ aspartic acid-β-cyclodextrin @ reduced graphene oxide (TiO_2 @ ACD @ RGO) composite photocatalysts by first reducing GO to RGO and then compounding it with aspartic acid-β-cyclodextrin and TiO_2, respectively. The photocatalytic efficiency of the prepared TiO_2@ ACD @ RGO for BPA degradation was significantly better than that of TiO_2 and TiO_2 @ RGO.

Herein, TiO_2-RGO was prepared for the degradation of different dyes (methyl orange, methylene blue and rhodamine B) in water using a one-pot hydrothermal method instead of a two-step process. The TiO_2-RGO was characterized using a multi-technical approach. The degradation performance of graphene addition on methyl orange dye was compared. The degradation of methyl orange, methylene blue and rhodamine B by TiO_2-RGO and the effect of the pH value of the reaction system on the photocatalytic degradation were investigated. The repetitive degradation properties of TiO_2-RGO were also explored. The present work opens a universal pathway for improving the photocatalytic performance of TiO_2.

2. Results and Discussion

2.1. The Effect of Graphene Oxide Addition on the Degradation of Methyl Orange Solution

The degradation effect of composites prepared with different amounts of graphene oxide on methyl orange solution is shown in Figure 1. Compared with the degradation effect of the catalyst without the addition of graphene oxide, the degradation efficiency of the methyl orange solution was significantly improved after the addition of graphene oxide (Figure 1a). On the one hand, it is due to the extremely strong electron transport ability of reduced graphene oxide, which can rapidly conduct photo-generated electrons and inhibit the compounding of photo-generated electrons and holes, thus increasing the concentration of hydroxyl radicals ($\cdot OH$) and superoxide ion radicals ($\cdot O^{2-}$), two strongly reducing and oxidizing radicals that can degrade dye molecules [25]. On the other hand, reduced graphene oxide has outstanding adsorption capacity, which improves the contact probability of pollutants with active substances [26–28].
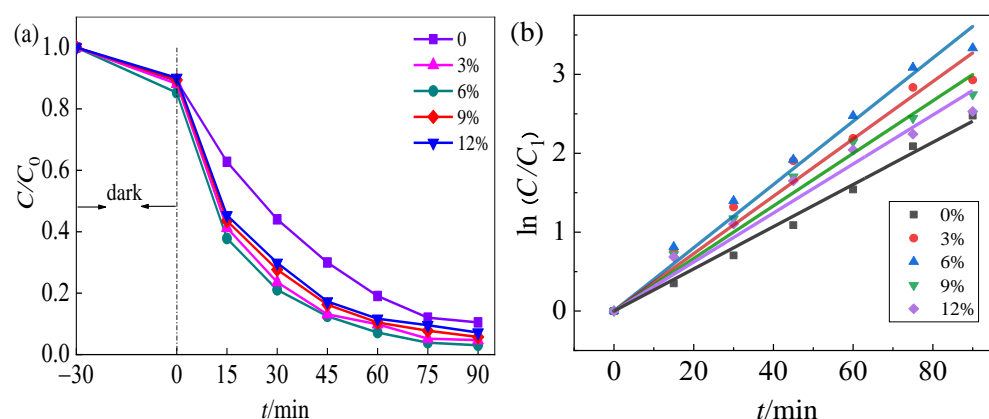
Figure 1. Degradation results of methyl orange by TiO_2-RGO with different GO contents (**a**) and its first-order kinetic analysis (**b**). C_0 is the initial concentration, C_1 is the concentration at 0 min.

It is worth noting that when the mass fraction of graphene oxide relative to titanium sulfate was 3%, the degradation rate of photocatalytic degradation for 90 min was 95.3%. When the mass fraction of graphene oxide relative to titanium sulfate was 6%, the photocatalytic degradation rate of 90 min was 6%, and the degradation rate of photocatalytic degradation for 90 min was 96.9%. When the mass fraction of graphene oxide relative to titanium sulfate increased to 12%, the degradation effect showed a downward trend instead, and the degradation rate after 90 min of reaction was 92.8%. This is because the reduced graphene oxide itself has no photocatalytic activity. When the content of reduced graphene oxide is too large, it will hinder the absorption of light energy by TiO_2 components, and cannot make enough TiO_2 to absorb light energy to transition to the excited state [29], thereby reducing the photocatalytic performance of the catalyst. Considering the degradation rate of dyes and the cost of composite materials with different graphene oxide contents, the optimal mass fraction of graphene oxide relative to titanium sulfate was determined to be 6% in this work.

To investigate the effect of reaction rate on the photocatalytic process, kinetic curves of each reaction were fitted (Figure 1b). The $\ln(C/C_1)$ of each reaction was found to have a good linear relationship with t, and the determination coefficients R^2 were all greater than 0.98 (Table 1), indicating that the photocatalytic reactions were consistent with the first-order reactions. The reaction rate k of TiO_2-RGO photocatalytic degradation of methyl orange was consistent with the change of degradation rate. The reaction rate of TiO_2-RGO photocatalytic degradation of methyl orange gradually increased with the addition of graphene oxide, but the reaction rate of photocatalytic reaction started to decrease when the mass fraction of graphene oxide relative to titanium sulfate exceeded 6%. In addition, the photocatalytic reaction rate of TiO_2-6% RGO was 1.501 times higher than that of TiO_2-0% RGO.

Table 1. Kinetic parameters of methyl orange degradation by TiO_2-RGO with different GO contents.

TiO_2-RGO	k/min^{-1}	R^2
TiO_2-0%RGO	0.0267	0.9967
TiO_2-%RGO	0.0364	0.9873
TiO_2-6%RGO	0.0401	0.9936
TiO_2-9%RGO	0.0333	0.9894
TiO_2-12%RGO	0.0311	0.9853

2.2. Characterization of TiO_2-RGO

When graphene is added during the preparation process, the graphene sheets can be interspersed between the TiO_2 particles so that the TiO_2 particles can be evenly distributed, improving the dispersibility, and are expected to further improve the photocatalytic per-

formance of the composite [30]. Figure 2 compares the SEM images of TiO_2-6%RGO and TiO_2-12%RGO. The particles of TiO_2-6%RGO are uniformly dispersed, have a relatively uniform particle size (~26 nm), and have a good morphology (Figure 2). The particles of TiO_2-12%RGO show obvious agglomeration, and the particle size varies greatly. When the graphene content is too high, the TiO_2-RGO appears to agglomerate during the preparation process, which also explains the abnormal phenomenon that the degradation rate of the TiO_2-RGO to methyl orange dye decreases.
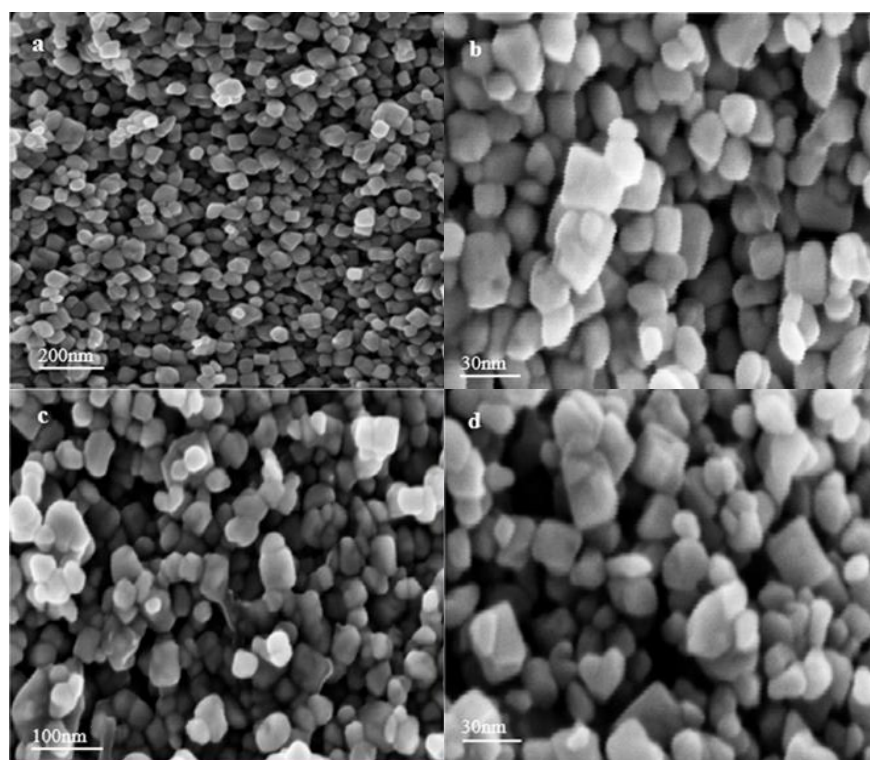

Figure 2. SEM images of TiO_2-RGO: (**a**,**b**) TiO_2-6%RGO, (**c**,**d**) TiO_2-12%RGO.

Figure 3a,b are the TEM images of TiO_2-6%RGO. It was observed that the graphene sheets with overlapping wrinkles are interspersed between the TiO_2 particles. The sample particles are relatively uniformly dispersed, and the particle size is relatively consistent. The TiO_2-12%RGO particles were disorderly stacked and agglomerated together (Figure 3c,d), which is consistent with the SEM results.

The XRD spectrum of GO shows a strong diffraction peak around 10.5°, and interestingly, there is no characteristic diffraction peak of graphite around 26°, indicating that the graphite powder is effectively oxidized and exfoliated (Figure 4a). TiO_2, TiO_2-6%RGO, and TiO_2-12%RGO have similar diffraction peaks, and the diffraction peaks at $2\theta = 25.3°$, 37.8°, 48.1°, 54°, 55.1°, and 62.7° are the diffraction peaks of the anatase phase TiO_2 {101}, {004}, {200}, {105}, {211}, {204} (Figure 4a), indicating that the addition of GO during the preparation process does not change the crystal structure of TiO_2. The XRD spectrum of TiO_2-6%RGO and TiO_2-12%RGO did not find the characteristic peak of GO at about 10.5°, which may show that GO has been reduced to RGO after the hydrothermal reaction. Interestingly, the characteristic diffraction peak of RGO was also not observed around $2\theta = 24.5°$. On the one hand, the reason for this phenomenon may be that the strong and sharp {101} crystal plane diffraction peak of anatase TiO_2 in the composite material at 25.3° shields the diffraction peak of RGO. On the other hand, it may be that the amount of GO added to the composite was small, and the diffraction intensity was too weak to be detected during the XRD characterization analysis [31].
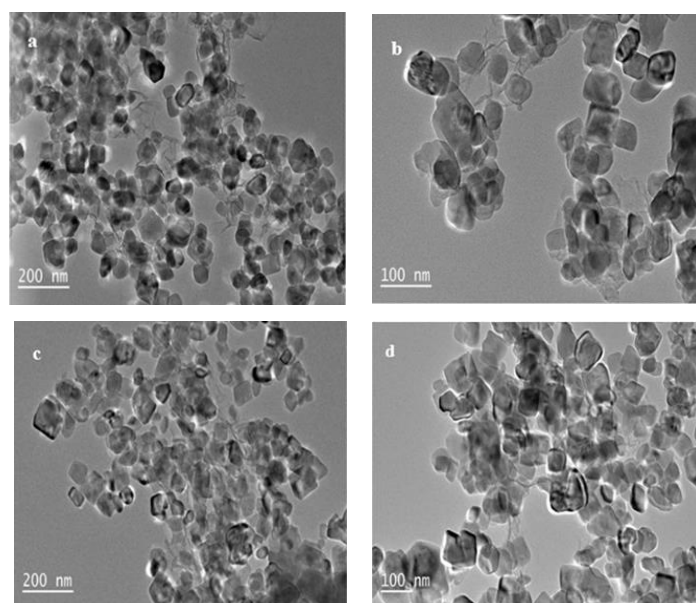
Figure 3. TEM images of TiO$_2$-RGO: (**a**,**b**) TiO$_2$-6%RGO, (**c**,**d**) TiO$_2$-12%RGO.
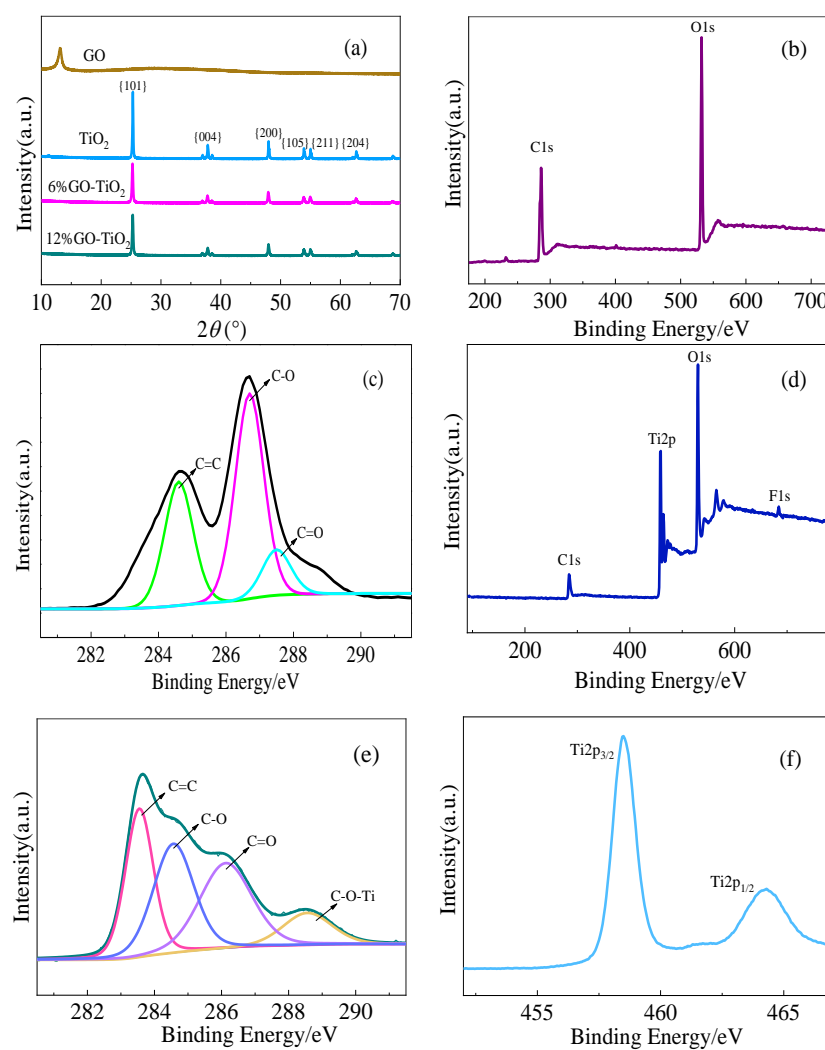

Figure 4. (**a**) XRD spectrum of GO, (**b**) XPS survey spectrum of GO, (**c**) C1s spectrum of GO, (**d**) XPS survey spectrum of TiO$_2$-6%RGO, (**e**) C1s spectrum of TiO$_2$-6%RGO, (**f**) Ti2p spectrum of TiO$_2$-6%RGO.

The XPS survey spectrum of GO in Figure 4b mainly shows two signal peaks, C1s and O1s, corresponding to 286 eV and 532 eV. The C1s signal peak can be fitted into three peaks, which are the signal peaks of C=C, C–O and C=O [32–34], and the corresponding binding energies of the fitted peaks are 284.61 eV, 286.7 eV and 287.5 eV, respectively (Figure 4c). There are mainly four signal peaks of C1s, Ti2p, O1s, and F1s in the XPS full spectrum of TiO_2-6%RGO, and the corresponding positions are 284 eV, 459 eV, 530 eV, and 684 eV, respectively (Figure 4d). The C1s signal peaks in TiO_2-6%RGO can be fitted to four signal peaks (Figure 4e), which are the signal peaks of C=C, C–O, C=O and C–O–Ti [35]. The C–O–Ti signal peak at 288.65 eV confirms that GO and TiO_2 in TiO_2-6%RGO are bound together by bonding [36]. The two signal peaks at 458.45 eV and 464.3 eV in Figure (Figure 4f) are the peaks of $Ti2p_{3/2}$ and $Ti2p_{1/2}$, respectively. These two signal peaks indicate that the Ti element in TiO_2-6%RGO exists in the form of Ti^{4+}.

Figure 5a illustrates the nitrogen adsorption–desorption isotherm of TiO_2 and TiO_2-6%RGO. Table 2 demonstrates that the addition of graphene can significantly increase the specific surface area and pore volume of TiO_2-RGO, which contributes to improving the contact probability of pollutants with the active substance. Figure 5b PL spectra of TiO_2 and TiO_2-6%RGO show that the PL intensity of TiO_2 is higher than that of TiO_2-6%RGO. This indicates that TiO_2 has a high photoinduced electron–hole pair complexation rate. Therefore, the reduced PL intensity of TiO_2-6%RGO suggests that the addition of GO significantly hinders the complexation of electrons and holes, which contributes to excellent photocatalytic activity.
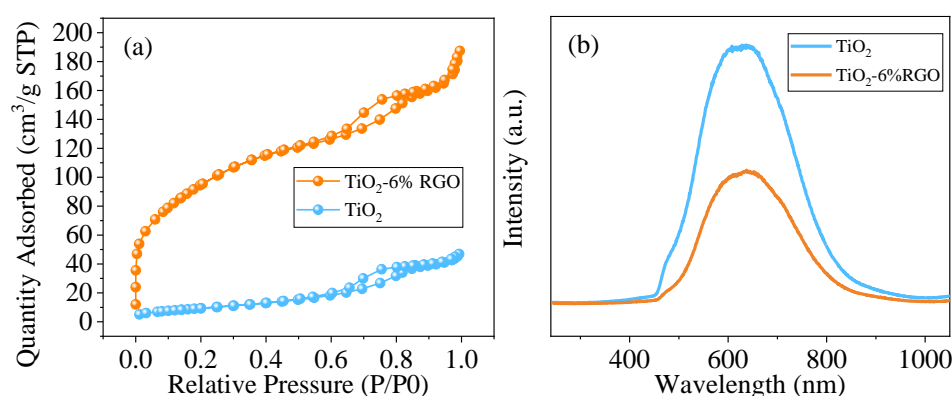
Figure 5. (**a**) Nitrogen adsorption–desorption isotherm of TiO_2 and TiO_2-6%RGO, (**b**) PL spectra of TiO_2 and TiO_2-6%RGO.

Table 2. The BET surface area and pore volume of TiO_2 and TiO_2-6%RGO.

Samples	BET Surface Area (m^2/g)	Pore Volume (cm^3/g)
TiO_2	35.68	0.0725
TiO_2-6%RGO	347.33	0.2898

2.3. The Effect of pH Value on the Degradation Effect of TiO_2-6%RGO

Figure 6a examines the degradation performance of TiO_2-6%RGO on methyl orange solutions under different pH environments. The pH of the methyl orange solution was adjusted with HCl and NaOH. Figure 6a highlights that the pH value has a great influence on the photocatalytic degradation effect of methyl orange solution. In the dark adsorption stage, the adsorption capacity of each reaction system increased with the decrease of pH value. The degradation performance under acidic conditions was significantly stronger than that under neutral and alkaline conditions. When pH = 2, the degradation rate of the reaction for 90 min was 93.1%. When pH = 4, the degradation rate of reaction for 75 min was 96.8%. When pH = 7, the degradation rate of the reaction for 90 min dropped to 89%. When pH = 10, the degradation rate of the reaction for 90 min was only 63%. The

kinetic fitting curves for the degradation of methyl orange by TiO_2-6%RGO at different pH environments are shown in Figure 5b, and the R^2 of the first-order kinetic fits were all greater than 0.99. The reaction rates of TiO_2-6%RGO degradation of methyl orange under different pH environments are shown in Table 3.
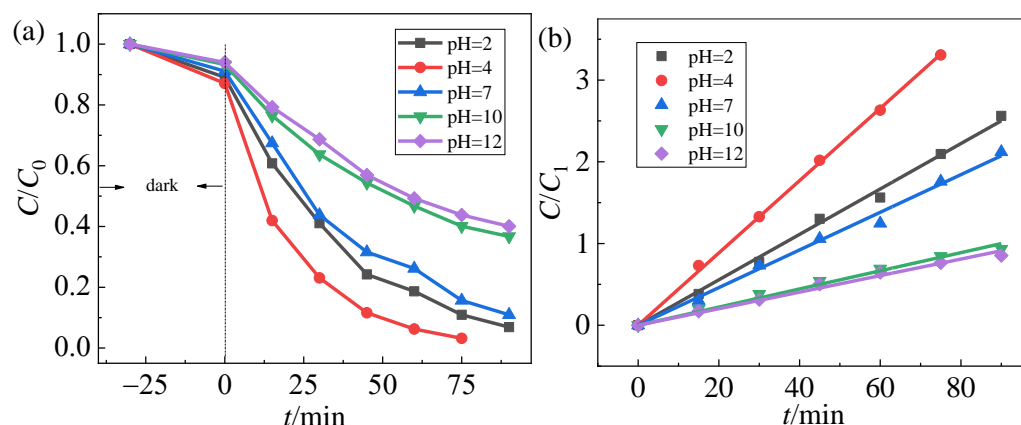
Figure 6. Degradation results of methyl orange at different pH values (**a**) and its first-order kinetic analysis (**b**).

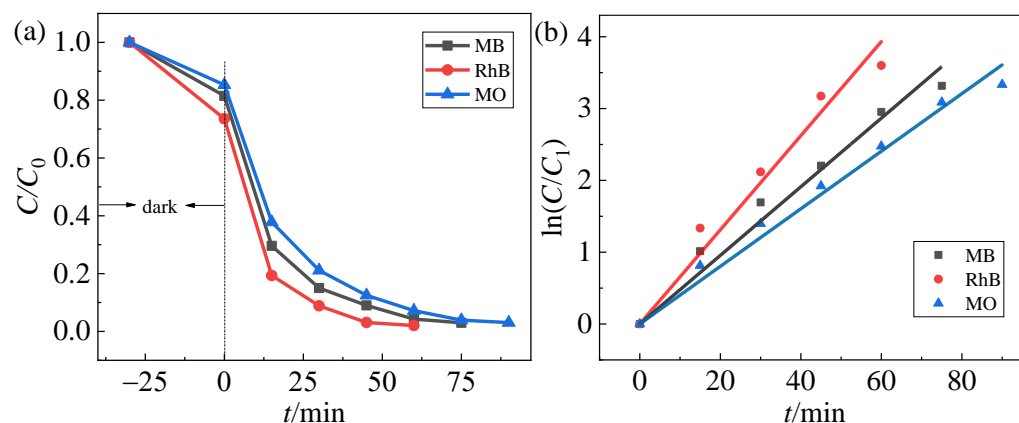**Table 3.** Kinetic parameters of TiO_2-6%RGO degradation of methyl orange solution at different pH values.

pH Value	k/min^{-1}	R^2
pH = 2	0.0278	0.9984
pH = 4	0.0442	0.9997
pH = 7	0.0230	0.9976
pH = 9	0.0111	0.9953
pH = 11	0.0101	0.9958

Since methyl orange is an anionic dye, when the reaction system is acidic, the enriched H^+ in the system makes the catalyst surface positively charged, which is more conducive to the adsorption of dye molecules. When the reaction system is alkaline, the enriched OH^- in the system inhibits the adsorption of dye molecules by the catalyst, which is not conducive to the photocatalytic degradation of methyl orange. Interestingly, the photocatalytic performance does not continuously improve with the decrease of pH value of the reaction system, as the degradation performance of pH = 2 is smaller than that of pH = 4. This is attributed to the fact that when the pH value is too low, the excess H^+ in the system is more easily reduced by photogenerated electrons, which inhibits the generation of active substances such as superoxide ion radicals ($\cdot O^{2-}$) [37], resulting in a decrease in the degradation efficiency.

2.4. Degradation Effect of TiO_2-6%RGO on Different Kinds of Dyes

To investigate the degradation effect of TiO_2-6%RGO on different kinds of dyes, three different dye solutions, methyl orange (MO), methylene blue (MB), and rhodamine B (RhB), were selected for photocatalytic degradation experiments. Methyl orange is an azo anionic dye commonly used as an acid–base indicator. Methylene blue is a cationic dye that is commonly used in the printing and dyeing industry. Rhodamine B is a fluorescent dye with a heterocyclic structure and high chroma in wastewater. Figure 7a shows that TiO_2-6%RGO has a faster degradation rate for methylene blue and rhodamine B solutions than methyl orange. The rhodamine B solution achieved a degradation rate of 81% within 15 min of the photocatalytic reaction, which was 1.3 times that of the methyl orange solution. The degradation rates of rhodamine B and methylene blue solutions were 97.9% and 97% at

60 min and 75 min, respectively, and the degradation rate of methyl orange solution at about 90 min was 96.9%. The kinetic fitting curves for the degradation of MO, MB and RhB by TiO_2-6%RGO are shown in Figure 7b, and the fitting results are consistent with the first-order kinetic reaction. The degradation rates of TiO_2-6%RGO for MO, MB and RhB dyes were 0.04008 min^{-1}, 0.04778 min^{-1} and 0.06554 min^{-1}, respectively (Table 4).

Figure 7. Degradation results of different dyes by TiO_2-6%RGO (**a**) and its first-order kinetic analysis (**b**).

**Table 4.** Kinetic parameters of different dye degradation by TiO_2-RGO.

Dyes	k/min^{-1}	R^2
MB	0.0478	0.9900
RhB	0.0655	0.9869
MO	0.0401	0.9936

In the dark adsorption stage, RhB has a lower concentration at the beginning of the photocatalytic reaction, as it can be more readily adsorbed by the oxygen-containing functional groups on the surface of TiO_2-6%RGO due to its greater polarity. The polarity of MO is slightly greater than that of methylene blue, but the dark adsorption capacity is lesser than that of methylene blue. This is possibly due to MB molecules containing more benzene rings and double bond structures, which are easily conjugated with the π electron-conjugated system of reduced graphene oxide to generate π-π conjugation, and the electrostatic attraction between positively charged and reduced graphene oxide makes it easier to be adsorbed [38]. The different adsorption amounts of the three dyes by TiO_2-6%RGO resulted in different degradation rates in the photocatalytic stage. In addition, rhodamine B is a fluorescent dye, which is more easily degraded under ultraviolet light.

2.5. Recycling Performance of TiO_2-6%RGO

To investigate the cyclic performance of the catalyst, a cyclic degradation experiment of methyl orange in solution with TiO_2-6%RGO was performed (Figure 8). The degradation rates of five cycles of operation were 96.9%, 96.7%, 95.3%, 94%, and 90.3%, respectively. The degradation effect of TiO_2-6%RGO on methyl orange showed a downward trend with the increase in the number of cycles, but it still maintained 93.2% of the initial degradation rate after five cycles. This can be attributed to the inevitable mass loss during the catalyst recovery process at the end of each degradation so that the amount of catalyst used in the subsequent cyclic degradation experiments was gradually reduced. In addition, in the photocatalytic degradation experiments, dye macromolecules or other impurity molecules remain on the catalyst surface and combine with the catalyst, which will lead to the weakening or even deactivation of the catalyst's activity, affecting its absorption of light energy [39].
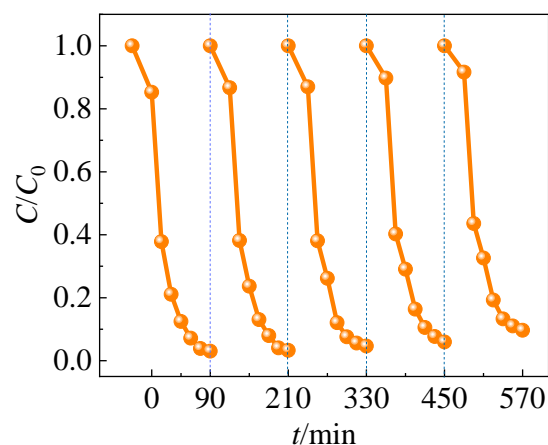
Figure 8. Cyclic degradation results of methyl orange by TiO_2-6%RGO.

Table 5 compares the degradation effects of the TiO_2-RGO with photocatalysts for similar applications. The TiO_2-RGO exhibits higher competitiveness, which has the potential to be applied for dye degradation in water.

Table 5. Comparison of dye degradation effects among various photocatalysts.

Photocatalyst	Degradation of Dyes	Degradation Rate (%)	Reference
Titanium dioxide	RhB	93.8	[40]
Ni/TiO_2	MB	95	[41]
Xanthan gum/titanium dioxide	MO	~89	[42]
THNF	MB	95.2	[43]
Sand/ZnO NRs/TiO_2 NRs (5 h)/GO_MWCNTs	MB	92.6	[44]
rGO/TiO_2	MB	92.7	[45]
RGO aerogel/TiO_2/MoS_2 composite	RhB	95	[46]
	MO	96.9	
TiO_2-RGO	RhB	97.9	This work
	MB	97	

3. Materials and Methods

3.1. Materials

Titanium sulfate (AR), hydrofluoric acid (AR), absolute ethanol (AR), methyl orange (MO, AR), methylene blue (MB, AR), rhodamine B (Rh B, AR), sodium nitrate (AR), sulfuric acid (mass fraction 98%), potassium permanganate (AR), glucose (AR), and graphite powder (AR) were purchased from Chemical Reagents Co., Ltd., Sinopharm, Beijing, China.

3.2. Preparation of Titanium Dioxide–Reduced Graphene Oxide Composites

The titanium dioxide–reduced graphene oxide composites were prepared by a one-step hydrothermal method. A total of 1.0 mL of HF was added dropwise to 40 mL of deionized water and stirred evenly. Then, 4.8 g of $Ti(SO_4)_2$ was added, ultrasonicated to make it completely dissolve, and this solution was used as solution A. A certain amount of GO powder and glucose powder (the mass ratio of GO to glucose is 1:3) was added to 30 mL of deionized water, and completely dissolved under ultrasonic conditions, and this solution was used as solution B. Solution A and solution B were mixed, stirred evenly, transferred to the lining of the reaction kettle, and reacted at 180 °C for 12 h. Then, the lower layer of precipitate was washed with deionized water several times until neutral, and finally dried and ground to obtain titanium dioxide–reduced graphene oxide composite material (TiO_2-RGO). The mass fractions of GO relative to $Ti(SO_4)_2$ in the composites were controlled to be 0, 3%, 6%, 9%, and 12%, which were named TiO_2-X%RGO, where X represents the mass fraction of GO relative to $Ti(SO_4)_2$.

3.3. Characterization

The equipment used was an X-ray photoelectron spectrometer (XPS), Escalab 250XI, Thermo Scientific, USA, an X-ray diffractometer (XRD), Bruker D8 Advance, Bruker, Germany, a scanning electron microscope (SEM), Hitachi S-4800, Japan, a transmission electron microscope, Hitachi H-7650, Japan, a physical adsorption analyser, ASAP 2460 Accelerated Surface Area and Porosimetry System, Micromeritics Instrument Corporation, USA and a fluorescence spectrometer (PL), FluoroMax-4, HORIBA Jobin Yvon, France.

3.4. Photocatalytic Degradation Experiments of Dyes by TiO$_2$-RGO

A total of 100 mg of TiO$_2$-RGO was added to 250 mL of dye solution at an initial concentration of 20 mg/L, and it was stirred for 30 min under a dark condition to reach the dynamic equilibrium of adsorption and desorption. Then, it was irradiated under a 500 W UV mercury lamp (the spectral range of the emitting light source is 341–455 nm) for photocatalytic degradation reaction. The reaction temperature in the photocatalytic reactor was kept constant by condensing water. The solution was taken at 15 min intervals, centrifuged, and the absorbance of the solution was measured by UV-Vis spectrophotometer with the supernatant. The TiO$_2$-RGO, obtained by centrifugation, washed several times with deionized water and then dried, can repeat the photocatalytic degradation experiments.

4. Conclusions

Titanium dioxide–reduced graphene oxide composites were prepared by a one-step hydrothermal method for the degradation of different dyes (methyl orange, methylene blue, and rhodamine B) in water. The graphene in the composite material can effectively inhibit the recombination of photogenerated electrons and holes, increase the contact area with dye molecules, and improve the photocatalytic performance of the material. The degradation rate of TiO$_2$-6%RGO for methyl orange at 15 min was 1.67 times higher than that of TiO$_2$. The degradation effect of TiO$_2$-6%RGO on methyl orange solution under different pH environments showed that a weakly acid environment was more favorable for the degradation of methyl orange dye. The degradation effect of TiO$_2$-6%RGO on different kinds of dyes was examined, and it showed better degradation performance on fluorescent dyes and anionic azoic dyes. Kinetic analysis indicated that the degradation of dye molecules by TiO$_2$-RGO is consistent with a first-order kinetic reaction. In addition, the photocatalytic degradation of methyl orange by TiO$_2$-6%RGO for 90 min could reach 96.9%, and 93.2% of the initial degradation rate could be maintained after five degradation cycles. This paper provides a practical avenue to design extremely efficient photocatalysts for dye degradation.

References

1. Wang, Z.H.; Liang, W.B.; Guo, X.; Liu, L. Inactivation of Scrippsiella trochoidea cysts by different physical and chemical methods: Application to the treatment of ballast water. *Mar. Pollut. Bull.* **2018**, *126*, 150–158. [CrossRef] [PubMed]
2. Al-Kaabi, M.A.; Zouari, N.; Dana, D.A.; Al-Ghouti, M.A. Adsorptive batch and biological treatments of produced water: Recent progresses, challenges, and potentials. *J. Environ. Manag.* **2021**, *290*, 112527. [CrossRef] [PubMed]
3. Rezvani, F.; Sarrafzadeh, M.H.; Ebrahimi, S.; Oh, H.M. Nitrate removal from drinking water with a focus on biological methods: A review. *Environ. Sci. Pollut. Res.* **2019**, *26*, 1124–1141. [CrossRef] [PubMed]
4. Camarillo, M.K.; Stringfellow, W.T. Biological treatment of oil and gas produced water: A review and meta-analysis. *Clean Technol. Environ. Policy* **2018**, *20*, 1127–1146. [CrossRef]

5. Qiu, N. The method of general heat treatment of waste water from metal manufacture based on photocatalysis. *Int. J. Environ. Pollut.* **2019**, *66*, 117–126. [CrossRef]

6. Pelosato, R.; Bolognino, I.; Fontana, F.; Sora, I.N. Applications of Heterogeneous Photocatalysis to the Degradation of Oxytetracy-cline in Water: A Review. *Molecules* **2022**, *27*, 2743. [CrossRef]

7. Du, C.Y.; Zhang, Z.; Yu, G.L.; Wu, H.P.; Chen, H.; Zhou, L.; Zhang, Y.; Su, Y.H.; Tan, S.Y.; Yang, L.; et al. A review of metal organic framework (MOFs)-based materials for antibiotics removal via adsorption and photocatalysis. *Chemosphere* **2021**, *272*, 129501. [CrossRef]

8. Yang, B.; Guan, B. Synergistic catalysis of ozonation and photooxidation by sandwich structured MnO_2-NH_2/GO/p-C_3N_4 on cephalexin degradation. *J. Hazard. Mater.* **2022**, *439*, 129540. [CrossRef]

9. Ebrahimbabaie, P.; Yousefi, K.; Pichtel, J. Photocatalytic and biological technologies for elimination of microplastics in water: Current status. *Sci. Total Environ.* **2022**, *806*, 150603. [CrossRef]

10. Fukugaichi, S. Fixation of Titanium Dioxide Nanoparticles on Glass Fiber Cloths for Photocatalytic Degradation of Organic Dyes. *ACS Omega* **2019**, *4*, 15175–15180. [CrossRef]

11. Huang, S.Y.; Chen, C.C.; Tsai, H.Y.; Shaya, J.; Lu, C.S. Photocatalytic degradation of thiobencarb by a visible light-driven MoS_2 photocatalyst. *Sep. Purif. Technol.* **2018**, *197*, 147–155. [CrossRef]

12. Elango, G.; Roopan, S.M. Efficacy of SnO_2 nanoparticles toward photocatalytic degradation of methylene blue dye. *J. Photochem. Photobiol. B-Biol.* **2016**, *155*, 34–38. [CrossRef] [PubMed]

13. Heidarpour, H.; Padervand, M.; Soltanieh, M.; Vossoughi, M. Enhanced decolorization of rhodamine B solution through simultaneous photocatalysis and persulfate activation over Fe/C_3N_4 photocatalyst. *Chem. Eng. Res. Des.* **2020**, *153*, 709–720. [CrossRef]

14. Padervand, M.; Ghasemi, S.; Hajiahmadi, S.; Rhimi, B.; Nejad, Z.G.; Karima, S.; Shahsavari, Z.; Wang, C.Y. Multifunctional Ag/AgCl/$ZnTiO_3$ structures as highly efficient photocatalysts for the removal of nitrophenols, CO_2 photoreduction, biomedical waste treatment, and bacteria inactivation. *Appl. Catal. A-Gen.* **2022**, *643*, 118794. [CrossRef]

15. Cheng, L.; Xiang, Q.J.; Liao, Y.L.; Zhang, H.W. CdS-Based photocatalysts. *Energy Environ. Sci.* **2018**, *11*, 1362–1391. [CrossRef]

16. Wen, Y.; Cao, S.; Fei, X.; Wang, H.; Wu, Z. One-step synthesized SO_4^{2-}-TiO_2 with exposed (001) facets and its application in selective catalytic reduction of NO by NH_3. *Chin. J. Catal.* **2018**, *39*, 771–778. [CrossRef]

17. Thompson, W.A.; Perier, C.; Maroto-Valer, M.M. Systematic study of sol-gel parameters on TiO_2 coating for CO_2 photoreduction. *Appl. Catal. B-Environ.* **2018**, *238*, 136–146. [CrossRef]

18. Shende, T.P.; Bhanvase, B.A.; Rathod, A.P.; Pinjari, D.V.; Sonawane, S.H. Sonochemical synthesis of Graphene-Ce-TiO_2 and Graphene-Fe-TiO_2 ternary hybrid photocatalyst nanocomposite and its application in degradation of crystal violet dye. *Ultrason. Sonochem.* **2018**, *41*, 582–589. [CrossRef]

19. Gao, Y.; Hu, M.; Mi, B.X. Membrane surface modification with TiO_2-graphene oxide for enhanced photocatalytic performance. *J. Membr. Sci.* **2014**, *455*, 349–356. [CrossRef]

20. Zabihi, F.; Ahmadian-Yazdi, M.R.; Eslamian, M. Photocatalytic Graphene-TiO_2 Thin Films Fabricated by Low-Temperature Ultrasonic Vibration-Assisted Spin and Spray Coating in a Sol-Gel Process. *Catalysts* **2017**, *7*, 136. [CrossRef]

21. Allen, M.J.; Tung, V.C.; Kaner, R.B. Honeycomb Carbon: A Review of Graphene. *Chem. Rev.* **2010**, *110*, 132–145. [CrossRef]

22. Bolotin, K.I.; Sikes, K.J.; Jiang, Z.; Klima, M.; Fudenberg, G.; Hone, J.; Kim, P.; Stormer, H.L. Ultrahigh electron mobility in suspended graphene. *Solid State Commun.* **2008**, *146*, 351–355. [CrossRef]

23. Tang, T.; Wang, T.; Gao, Y.; Xiao, H.; Xu, J.H. Two step method for preparing TiO_2/Ag/rGO heterogeneous nanocomposites and its photocatalytic activity under visible light irradiation. *J. Mater. Sci.-Mater. Electron.* **2019**, *30*, 8471–8478. [CrossRef]

24. Wang, G.H.; Dai, J.L.; Luo, Q.Y.; Deng, N.S. Photocatalytic degradation of bisphenol A by TiO_2@aspartic acid-beta-cyclodextrin@reduced graphene oxide. *Sep. Purif. Technol.* **2021**, *254*, 117574. [CrossRef]

25. Jing, L.; Yang, Z.Y.; Zhao, Y.F.; Zhang, Y.X.; Guo, X.; Yan, Y.M.; Sun, K.N. Ternary polyaniline-graphene-TiO_2 hybrid with enhanced activity for visible-light photo-electrocatalytic water oxidation. *J. Mater. Chem. A* **2014**, *2*, 1068–1075. [CrossRef]

26. Xu, W.L.; Chen, S.; Zhu, Y.N.; Xiang, X.X.; Bo, Y.Q.; Lin, Z.M.; Wu, H.; Liu, H. Preparation of hyperelastic graphene/carboxymethyl cellulose composite aerogels by ambient pressure drying and its adsorption applications. *J. Mater. Sci.* **2020**, *55*, 10543–10557. [CrossRef]

27. ASham, Y.W.; Notley, S.M. Adsorption of organic dyes from aqueous solutions using surfactant exfoliated graphene. *J. Environ. Chem. Eng.* **2018**, *6*, 495–504.

28. Chen, Y.Y.; Wang, L.H.; Sun, H.Y.; Zhang, D.D.; Zhao, Y.P.; Chen, L. Self-assembling TiO_2 on aminated graphene based on adsorption and catalysis to treat organic dyes. *Appl. Surf. Sci.* **2021**, *539*, 147889. [CrossRef]

29. Wang, D.T.; Li, X.; Chen, J.F.; Tao, X. Enhanced Visible-Light Photoelectrocatalytic Degradation of Organic Contaminants at Iodine-Doped Titanium Dioxide Film Electrode. *Ind. Eng. Chem. Res.* **2012**, *51*, 218–224. [CrossRef]

30. Adamu, H.; Dubey, P.; Anderson, J.A. Probing the role of thermally reduced graphene oxide in enhancing performance of TiO_2 in photocatalytic phenol removal from aqueous environments. *Chem. Eng. J.* **2016**, *284*, 380–388. [CrossRef]

31. Liu, J.C.; Wang, L.; Tang, J.C.; Ma, J.L. Photocatalytic degradation of commercially sourced naphthenic acids by TiO_2-graphene composite nanomaterial. *Chemosphere* **2016**, *149*, 328–335. [CrossRef] [PubMed]

32. Wan, C.; Peng, T.J.; Sun, H.J.; Huang, Q. Preparation and Humidity-Sensitive Properties of Graphene Oxide in Different Oxidation Degree. *Chin. J. Inorg. Chem.* **2012**, *28*, 915–921.

33. YMin, L.; Zhang, K.; Zhao, W.; Zheng, F.C.; Chen, Y.C.; Zhang, Y.G. Enhanced chemical interaction between TiO_2 and graphene oxide for photocatalytic decolorization of methylene blue. *Chem. Eng. J.* **2012**, *193*, 203–210.
34. Chou, P.W.; Wang, Y.S.; Lin, C.C.; Chen, Y.J.; Cheng, C.L.; Wong, M.S. Effect of carbon and oxygen on phase transformation of titania films during annealing. *Surf. Coat. Technol.* **2009**, *204*, 834–839. [CrossRef]
35. di Valentin, C.; Pacchioni, G.; Selloni, A. Theory of carbon doping of titanium dioxide. *Chem. Mater.* **2005**, *17*, 6656–6665. [CrossRef]
36. Ren, W.J.; Ai, Z.H.; Jia, F.L.; Zhang, L.Z.; Fan, X.X.; Zou, Z.G. Low temperature preparation and visible light photocatalytic activity of mesoporous carbon-doped crystalline TiO_2. *Appl. Catal. B-Environ.* **2007**, *69*, 138–144. [CrossRef]
37. CGuo, S.; Ge, M.; Liu, L.; Gao, G.D.; Feng, Y.C.; Wang, Y.Q. Directed Synthesis of Mesoporous TiO2 Microspheres: Catalysts and Their Photocatalysis for Bisphenol A Degradation. *Environ. Sci. Technol.* **2010**, *44*, 419–425.
38. Zhang, Q.L.; Qin, Z.; Liu, Y.Z.; Ting, Y.T.; Zhang, J.W.; Zeng, G.P. Adsorption kinetics and photocatalytic activity of grapheneoxide-TiO2 composites for three dyes. *Chem. Ind. Eng. Prog.* **2019**, *38*, 2870–2879.
39. Ali, I. New Generation Adsorbents for Water Treatment. *Chem. Rev.* **2012**, *112*, 5073–5091. [CrossRef]
40. Kiwaan, H.A.; Atwee, T.M.; Azab, E.A.; El-Bindary, A.A. Photocatalytic degradation of organic dyes in the presence of nanostructured titanium dioxide. *J. Mol. Struct.* **2020**, *1200*, 127115. [CrossRef]
41. Sadia, M.; Naz, R.; Khan, J.; Zahoor, M.; Ullah, R.; Khan, R.; Naz, S.; Almoallim, H.S.; Alharbi, S.A. Metal doped titania nanoparticles as efficient photocatalyst for dyes degradation. *J. King Saud Univ. Sci.* **2021**, *33*, 101312. [CrossRef]
42. Inamuddin. Xanthan gum/titanium dioxide nanocomposite for photocatalytic degradation of methyl orange dye. *Int. J. Biol. Macromol.* **2019**, *121*, 1046–1053. [CrossRef] [PubMed]
43. Jafri, N.N.M.; Jaafar, J.; Alias, N.H.; Samitsu, S.; Aziz, F.; Salleh, W.N.W.; Yusop, M.Z.M.; Othman, M.H.D.; Rahman, M.A.; Ismail, A.F.; et al. Synthesis and Characterization of Titanium Dioxide Hollow Nanofiber for Photocatalytic Degradation of Methylene Blue Dye. *Membranes* **2021**, *11*, 581. [CrossRef]
44. Idris, N.J.; Bakar, S.A.; Mohamed, A.; Muqoyyanah, M.; Othman, M.H.D.; Mamat, M.H.; Ahmad, M.K.; Birowosuto, M.D.; Soga, T. Photocatalytic performance improvement by utilizing GO_MWCNTs hybrid solution on sand/ZnO/TiO2-based photocatalysts to degrade methylene blue dye. *Environ. Sci. Pollut. Res.* **2021**, *28*, 6966–6979. [CrossRef] [PubMed]
45. Kocijan, M.; Curkovic, L.; Bdikin, I.; Otero-Irurueta, G.; Hortigueela, M.J.; Goncalves, G.; Radosevic, T.; Vengust, D.; Podlogar, M. Immobilised rGO/TiO2 Nanocomposite for Multi-Cycle Removal of Methylene Blue Dye from an Aqueous Medium. *Appl. Sci.* **2022**, *12*, 385. [CrossRef]
46. Zhang, Y.J.; Qi, H.J.; Zhang, L.; Wang, Y.; Zhong, L.L.; Zheng, Y.G.; Wen, X.; Zhang, X.M.; Xue, J.Q. A RGO aerogel/TiO2/MoS2 composite photocatalyst for the removal of organic dyes by the cooperative action of adsorption and photocatalysis. *Environ. Sci. Pollut. Res.* **2022**, *29*, 8980–8995. [CrossRef] [PubMed]